

Study of the superconducting gap in $R\text{Ni}_2\text{B}_2\text{C}$ ($R = \text{Y}, \text{Lu}$) single crystals by inelastic light scattering

In-Sang Yang

*Department of Physics, Ewha Womans University, 120-750, Seoul, Korea
and Materials Research Laboratory, Department of Physics, University of Illinois at Urbana-Champaign, Urbana, Illinois 61801*

M. V. Klein and S. L. Cooper

Materials Research Laboratory, Department of Physics, University of Illinois at Urbana-Champaign, Urbana, Illinois 61801

P. C. Canfield

Ames Laboratory, Department of Physics and Astronomy, Iowa State University, Ames, Iowa 50011

B. K. Cho* and Sung-Ik Lee

*National Creative Research Initiative Center for Superconductivity, Department of Physics,
Pohang University of Science and Technology, 790-390 Pohang, Korea*

(Received 28 February 2000)

Superconductivity-induced changes in the electronic Raman-scattering response were observed for the $R\text{Ni}_2\text{B}_2\text{C}$ ($R = \text{Y}, \text{Lu}$) system in different scattering geometries. In the superconducting state, 2Δ -like peaks were observed in A_{1g} , B_{1g} , and B_{2g} spectra from single crystals. The peaks in A_{1g} and B_{2g} symmetries are significantly sharper and stronger than the peak in B_{1g} symmetry. The temperature dependence of the frequencies of the 2Δ -like peaks shows typical BCS-type behavior, but the apparent values of the 2Δ gap are strongly anisotropic for both systems. In addition, for both $\text{YNi}_2\text{B}_2\text{C}$ and $\text{LuNi}_2\text{B}_2\text{C}$ systems, there exists reproducible scattering strength below the 2Δ gap which is roughly linear to the frequency in B_{1g} and B_{2g} symmetries. This discovery of scattering below the gap in nonmagnetic borocarbide superconductors, which are thought to be conventional BCS-type superconductors, is a challenge for current understanding of superconductivity in this system.

I. INTRODUCTION

The rare-earth borocarbides are believed to be conventional BCS-type superconductors¹ with a number of interesting properties that are not fully understood. Borocarbides are similar to intermetallic superconductors such as V_3Si and Nb_3Sn in that they have a relatively strong electron-phonon coupling constant and a moderately large density of states at the Fermi level.² While it is generally agreed that the electron-phonon interaction is the underlying mechanism for superconductivity in these systems, the responsible phonons are claimed to be either a high-energy phonon (boron A_{1g} near 850 cm^{-1})³ or a low-energy soft-mode phonon.⁴ Additionally, the borocarbides have relatively simple tetragonal crystal structure, yet they show a variety of physical properties that have been active research topics over the past years. For example, some of the borocarbides exhibit magnetic ordering and superconductivity at around the same temperature, offering the possibility of studying the interplay between superconductivity and magnetism.⁵

Even the nonmagnetic rare-earth borocarbides $R\text{Ni}_2\text{B}_2\text{C}$ ($R = \text{Y}, \text{Lu}$) show rich superconducting phenomena, such as anisotropic upper critical fields and angular dependence of in-plane magnetization,⁶ a hexagonal-to-square vortex lattice transition,⁷⁻⁹ and phonon-softening at a finite wave vector where strong Fermi-surface nesting is suggested.¹⁰ The results of inelastic neutron-scattering measurements¹⁰ are on

soft $q \neq 0$ phonons, which would not be detected using Raman spectroscopy.

A study of the low-energy excitation spectra would clearly lead to a more complete understanding of the electronic interaction in these systems. The superconducting gap has been a major subject of research in superconductivity. Up to now, the gap in borocarbides has been studied by tunneling spectroscopy¹¹ and infrared (IR) reflectivity¹² which are insensitive to the wave-vector space dependence of the gap. Electronic Raman spectroscopy is sensitive to the wave-vector dependence of the gap. When the optical penetration depth exceeds the superconducting coherence length, it yields a susceptibility for two quasiparticles of essentially zero total wave vector. The quasiparticles that contribute to the response are those with wave vectors close to the Fermi surface for which the Raman vertex has a large modulus squared. This vertex equals the projection onto the polarization vectors of the incident and scattered photons of a tensor closely related to the inverse effective-mass tensor. Manipulation of the polarization vectors changes the Raman symmetry and selectively probes the gap near certain regions of the Fermi surface.¹³ Raman spectroscopy studies have played an important role in understanding superconductivity of conventional¹⁴ and exotic superconductors.¹⁵ For example, superconductivity-induced redistribution of the electronic continua of the high- T_c superconductors led to important clues as to the d -wave nature of the order parameter. However, there remain unsolved puzzles regarding different val-

ues of the 2Δ peak positions in different scattering geometries, the power-law behavior of the scattering response below 2Δ and its relation to the d -wave nature of the order parameter, and to the role of impurities.

Until now there has been only one kind of ‘‘conventional’’ superconductor ($A15$) whose gap was measured by electronic Raman, while there are numerous oxide superconductors measured by the same technique. In other words, we do not really know how the conventional superconductors behave in the electronic Raman studies. Without a sound background for comparison, many of the studies of ‘‘unconventional’’ behavior of the exotic superconductors would be meaningless. From a number of aspects (including our own measurements), borocarbides seem to behave conventionally. Thus borocarbides would be suitable choice of superconductor for investigation using electronic Raman spectroscopy.

In this paper, we report an observation of clear redistribution of the electronic continua in different scattering geometries in the $R\text{Ni}_2\text{B}_2\text{C}$ ($R = \text{Y, Lu}$) borocarbides in the superconducting state. 2Δ -like peaks were observed in the superconducting state in A_{1g} , B_{1g} , and B_{2g} Raman symmetry from single crystals. The peaks in A_{1g} and B_{2g} symmetries are significantly sharper and stronger than the peak in B_{1g} symmetry. The temperature dependence of the frequencies of the peaks shows typical BCS-type behavior of the superconducting gap, but the apparent values of the 2Δ gap are strongly anisotropic for both systems. In contrast to what we normally expect from conventional superconductors, we find reproducible scattering strength below the 2Δ -like peak in all the scattering geometries. This Raman measurement shows finite scattering below the gaplike peaks of the ‘‘conventional’’ superconductors. Previous measurements on $A15$'s were too noisy to detect any finite scattering below the gap.¹⁴

II. EXPERIMENT

All the samples measured in this work were single crystals grown by the flux-growth method.^{5,16} Samples were characterized by various measurements, including resistivity versus temperature, magnetization versus temperature, and neutron scattering.¹⁷ The crystal structure of $R\text{Ni}_2\text{B}_2\text{C}$ is tetragonal body-centered space group $I4/mmm$, and phononic Raman analyses have been made earlier.¹⁸ Raman spectra were obtained in a pseudobackscattering geometry using a custom-made subtractive triple-grating spectrometer designed for very small Raman shifts and ultralow intensities.¹⁹ 3 mW of 6471-Å Kr-ion laser light was focused onto a spot of $100 \times 100 \mu\text{m}^2$, which results in heating of the spot above the temperature of the sample environment. The temperature of the spot on the sample surface was estimated by solving the heat-diffusion equation. ΔT , the rise in temperature, is proportional to the inverse of the thermal conductivity of the sample. ΔT is largest at lowest temperature because the thermal conductivity is smaller at lower temperatures.²⁰ The estimated ΔT is 2.7 K at 4 K and 0.9 K at 14 K for the case of $\text{YNi}_2\text{B}_2\text{C}$ single crystal. The ambient temperature at which the Raman continua begin to show the redistribution was determined to be 14 K, which is in agreement with this estimation. All the spectra have been corrected for the Bose

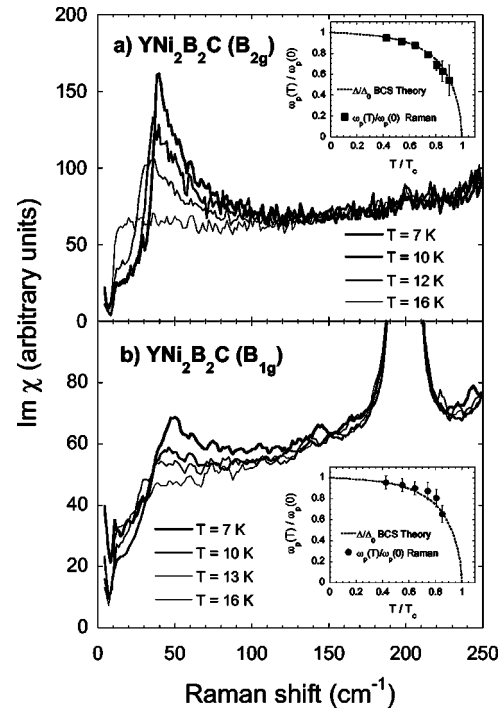


FIG. 1. The Raman spectra of $\text{YNi}_2\text{B}_2\text{C}$ ($T_c = 15.3$ K, $\Delta T_c = 0.4$ K) in B_{2g} and B_{1g} scattering geometries at various temperatures. The insets show $\omega_p/\omega_p(0)$, the normalized frequencies of the peaks as functions of the reduced temperature T/T_c . Determining $\omega_p(0)$ is explained in the text. The dotted curves are for Δ/Δ_0 predicted by the BCS theory. The error in ω_p comes from the broadness of the peak feature especially near $T = T_c$. Uncertainty in the reduced temperature is smaller than the size of the symbols.

factor. They therefore are proportional to the imaginary part of the Raman susceptibility.

III. RESULTS AND DISCUSSION

Superconductivity-induced changes in the B_{2g} and B_{1g} spectra of $\text{YNi}_2\text{B}_2\text{C}$ taken at different temperatures are shown in Fig. 1. The quality of the sample surfaces was good enough that Raman spectra could be taken down to $\sim 10 \text{ cm}^{-1}$. Sharp drops of the spectra below 10 cm^{-1} (for B_{2g} and B_{1g}) or 20 cm^{-1} (for A_{1g}) are due to cutoff of the filtering stage, and the sharp rises near zero frequency are due to the laser line (6471 Å). The relative strengths of the spectra in different scattering geometries are meaningful although the absolute values of the scattering strength are in arbitrary units in all the figures. In the superconducting state ($T \approx 7$ K), the spectra show a clear redistribution of the scattering weight: depletion of the weight at low frequencies ($\leq 40 \text{ cm}^{-1}$) and the accumulation of the weight above $\sim 40 \text{ cm}^{-1}$, resulting in sharp gaplike peaks in both B_{2g} and B_{1g} symmetries. The gaplike feature is more prominent and sharper in B_{2g} symmetry than in B_{1g} symmetry. The sharpness of the B_{2g} peak suggests that its origin may be different from that of B_{1g} .

The peak at 200 cm^{-1} is the Ni B_{1g} phonon mode, the height of which (1250 on the same scale) is much stronger than the B_{1g} electronic Raman peaks. Previous Raman measurements on borocarbides concentrated mainly on phononic peaks,¹⁸ and the gap features were not observed in earlier

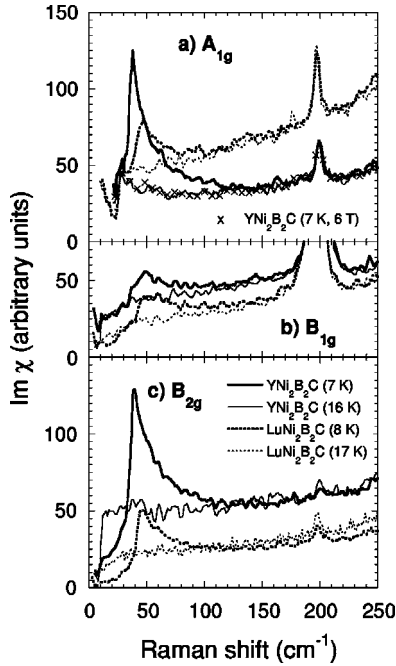


FIG. 2. Raman spectra in A_{1g} , B_{1g} , and B_{2g} geometries of $\text{YNi}_2\text{B}_2\text{C}$ ($T_c = 15.3$ K, $\Delta T_c = 0.4$ K) and $\text{LuNi}_2\text{B}_2\text{C}$ ($T_c = 15.7$ K, $\Delta T_c = 0.4$ K) in superconducting states and in normal states. The A_{1g} spectra were taken using left-circularly polarized light in both excitation and detection (left-left geometry). The spectrum denoted by x was taken at a magnetic field of 6 T. The peaks at ~ 200 cm^{-1} in the A_{1g} spectra are leakage of the strong B_{1g} phonon due to slight misalignment of the polarizer and analyzer.

electronic Raman measurements.²¹ Electronic Raman spectra from borocarbides are so weak that a sensitive spectrometer with good stray-light rejection is required.

The peak frequency ω_p , read from graphs, of the peak feature taken at 7 K is normalized in such a way that its normalized value is the same as the value of the reduced superconducting gap $\Delta(T=7\text{ K})/\Delta_0 (=0.95)$ in the BCS theory, where $\Delta_0 = \Delta(T=0)$, at the reduced temperature of 0.45 ($=7/15.5$). $\omega_p(0)$, the values of the peak frequency in the limit of 0 K thus obtained are 40.1 cm^{-1} for B_{2g} and 48.9 cm^{-1} for B_{1g} . $\omega_p/\omega_p(0)$, the normalized frequencies of the peaks of the peak features as functions of the reduced temperatures follow the curve for $\Delta(T)/\Delta_0$ predicted by the BCS theory as shown in the insets of the figure. This suggests that the peak features arise due to opening of the superconducting gap and provides some evidence that borocarbides are conventional BCS-type superconductors.

One of the advantages of the borocarbide superconductors is that their upper critical fields ($H_{c2} \leq 6T$ at 6 K) can be easily reached by using commercial superconducting magnets. We applied strong magnetic fields (up to 7 T) parallel to c axis and investigated the effects on these gaplike features of both $\text{YNi}_2\text{B}_2\text{C}$ and $\text{LuNi}_2\text{B}_2\text{C}$ crystals at low temperatures. The gaplike features were completely suppressed by the strong magnetic fields, confirming that these features are indeed induced by superconductivity [see Fig. 2(a)]. Full analysis of the dependence on magnetic fields of the peak frequencies and the features below the gap will be presented in an additional manuscript.

Unlike other gap-probing measurements such as tunneling experiments and x-ray photoemission spectroscopy (XPS), Raman spectroscopy is able to measure the anisotropy of the gap at a high resolution of a few meV. In addition, electronic Raman spectroscopy has an advantage over infrared spectroscopy¹² in studying the gap of superconductors in their clean limit. Figure 2 shows Raman spectra in A_{1g} , B_{1g} , and B_{2g} geometries of $\text{YNi}_2\text{B}_2\text{C}$ and $\text{LuNi}_2\text{B}_2\text{C}$ in superconducting states and in normal states. Spectra in E_g geometry were difficult to acquire from either fractured or polish-then-etched ac surfaces, even if those surfaces were optically flat. The A_{1g} spectra reflect weighted average of the Fermi surface with a weighting function of $k_x^2 + k_y^2$ symmetry; the B_{1g} spectra, $k_x^2 - k_y^2$ symmetry; and the B_{2g} spectra, $k_x k_y$ symmetry. The polarizations used were such that a contribution of A_{2g} symmetry is possible in all three cases; however, the A_{2g} spectrum is expected to be negligible. The most apparent phenomenon is the anisotropy in the intensity and sharpness of the gaplike features. The A_{1g} and B_{2g} peaks are significantly stronger and sharper than the B_{1g} peak. Together with the smaller values of the positions of the A_{1g} and B_{2g} peaks than that of B_{1g} peak as detailed below, this suggests that the sharp A_{1g} and B_{2g} peaks might be a reflection of collective modes. Further investigation is necessary to clarify the origin of the peaks.

The B_{1g} gap energy is considerably larger than the B_{2g} gap energy signifying perhaps that the gap parameters are anisotropic for both $\text{YNi}_2\text{B}_2\text{C}$ and $\text{LuNi}_2\text{B}_2\text{C}$. The apparent gap anisotropy is more pronounced in $\text{YNi}_2\text{B}_2\text{C}$ than in $\text{LuNi}_2\text{B}_2\text{C}$. The values extrapolated at $T=0$ are $\Delta_0(A_{1g}) = 2.5$ meV ($2\Delta_0/kT_c = 3.7$), $\Delta_0(B_{1g}) = 3.0$ meV ($2\Delta_0/kT_c = 4.5$), and $\Delta_0(B_{2g}) = 2.5$ meV ($2\Delta_0/kT_c = 3.7$) for $\text{YNi}_2\text{B}_2\text{C}$, while $\Delta_0(A_{1g}) = 3.0$ meV ($2\Delta_0/kT_c = 4.4$), $\Delta_0(B_{1g}) = 3.3$ meV ($2\Delta_0/kT_c = 4.8$), and $\Delta_0(B_{2g}) = 3.1$ meV ($2\Delta_0/kT_c = 4.5$) for $\text{LuNi}_2\text{B}_2\text{C}$. These values are different from the values from other measurements.^{11,12} For instance, an IR reflectivity measurement reports $\Delta_0 = 3.46$ meV for polycrystalline $\text{YNi}_2\text{B}_2\text{C}$ and $\Delta_0 = 2.68$ meV for single crystal $\text{LuNi}_2\text{B}_2\text{C}$.¹²

There is reproducible spectral weight below the 2Δ peak in both symmetries for both $\text{YNi}_2\text{B}_2\text{C}$ and $\text{LuNi}_2\text{B}_2\text{C}$ systems. Special care was taken in studying the features below the gap: Samples with high quality surfaces were selected; higher resolution and longer exposure times were employed. Figure 3 shows Raman spectra of $\text{YNi}_2\text{B}_2\text{C}$ (B^{10} isotope) in B_{2g} and B_{1g} symmetries. In this particular case, the cutoff of the filter state in the spectrometer was 6 cm^{-1} . As far as the spectral weight below the 2Δ peak is concerned, samples with different boron isotopes give the same results. Both B_{2g} and B_{1g} spectra show finite Raman scattering below the gap and it appears to be roughly linear to the Raman frequency below 30 cm^{-1} . For the B_{2g} spectrum, there is an abrupt slope change at about 30 cm^{-1} . Similar linear-in-frequency behavior was observed in the spectra of $\text{LuNi}_2\text{B}_2\text{C}$ below 35 cm^{-1} . The possibility of instrumental broadening is ruled out by measuring the spectral widths of Kr-ion plasma lines, which are about 2.5 cm^{-1} in the spectral range of these measurements.

Such a feature below the gap could rise from different causes. We eliminate the possibilities of (i) an extrinsic

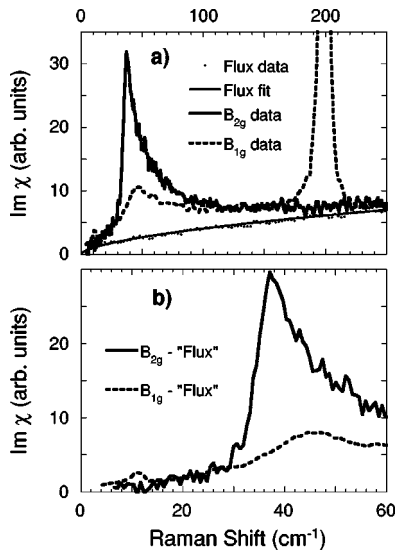


FIG. 3. (a) Raman spectra of superconducting $\text{YNi}_2\text{B}_2\text{C}$ (B^{10} isotope, $T_c=15.3$ K, $\Delta T_c=0.4$ K) in B_{2g} (solid line) and B_{1g} (dashed line) symmetries. Raman spectra of the flux phase are shown as solid dots along with a fit (thin line). (b) Assuming that all the Raman intensity at 250 cm^{-1} is from the flux phase, the “intrinsic” Raman spectra of B_{2g} (solid line) and B_{1g} (dashed line) are obtained by subtracting the “flux” contribution. This would be underestimation of the true intrinsic spectra.

phase on the sample surfaces and (ii) inhomogeneity of the probing laser beam, and argue that this sub-gap feature is intrinsic to the borocarbide superconductors. This would constitute a definitive experimental observation of finite Raman scattering below the gap feature for the “conventional” superconductors. Previous measurements on $A15$ compounds were simply too noisy to detect any finite scattering below the gap.¹⁴

(i) The borocarbide single crystals do have extrinsic phases, mostly from the flux. In our measurements, we were able to avoid such flux phases. If the sub-gap feature were due to an extrinsic phase, the intensity of the sub-gap feature would be dependent on the measurement conditions, e.g., dependent on the fraction of flux under the exciting focussed laser spot. All the spectra showed the same intensity, independent of where the spot was located. X-ray photoemission spectroscopy (XPS) analyses show that the flux phase on the surface of the single crystals is Ni_3B or Ni_3BC . Scanning electron microscopy (SEM) did not reveal any small-grained structures on the surface or edges of the single crystals. Auger analyses did not show any fine structures either. Furthermore, they showed that chemical compositions did not vary significantly from point to point on the surface. All these analyses suggest that there is no fine-grained extrinsic phase contributing to the Raman spectra. In addition, we actually measured the Raman spectra of the flux phase itself [Fig. 3(a)]. Even if all the Raman intensity above the gap feature is assumed to be due to the flux (overestimation of the flux contribution), a finite Raman intensity below the peak feature is always obtained (underestimation of the intrinsic contribution), as shown in Fig. 3(b).

(ii) An experimental situation where part of the measured spot is normal (or close to the normal state) and another part

is deep in the superconducting state due to inhomogeneity of the laser spot could lead to finite scattering intensity below the gap. This scenario is excluded as follows: (i) In the measurements, spatial filtering the excitation laser source was used to make the incident beam as homogeneous as possible. (ii) We used several different laser intensities and confirmed the same feature below the gap. The overall intensity scaled with the incident power as long as the heating effect was small, so that the temperature of the measured spot remained well below T_c . (iii) The sharpness of the B_{2g} peak itself indicates that the actual temperature of the measured spot is quite uniform and well below T_c . Otherwise, we should not be able to see such a steep slope below the B_{2g} peak. Therefore, we believe that the finite Raman intensity below the peak feature is intrinsic.

Cuprate superconductors show finite Raman response below the 2Δ -like peak even in the superconducting state.¹⁵ The lack of the complete suppression of the Raman response below the 2Δ peak has been regarded as evidence that the superconducting gap function of cuprates has nodes where the gap vanishes.²² In simple BCS picture no density of states is allowed below the superconducting gap; thus no Raman scattering beyond small smearing effects is expected below the gap in BCS-type superconductors. However, in this work, finite Raman scattering is observed below the gap of borocarbides.

The underlying mechanism that gives rise to the linear-in-frequency behavior below the 2Δ gap for the borocarbides, which are believed to be conventional BCS-type superconductors, needs to be clarified further.

IV. CONCLUSION

In conclusion, sharp redistributions of the continuum of Raman spectra were observed in different geometries for the $R\text{Ni}_2\text{B}_2\text{C}$ ($R=\text{Y, Lu}$) systems upon going into the superconducting states. 2Δ -like features were observed in the A_{1g} , B_{1g} , and B_{2g} spectra of the $R\text{Ni}_2\text{B}_2\text{C}$ ($R=\text{Y, Lu}$) single crystals in the superconducting states. The peak features in A_{1g} and B_{2g} geometry are sharper and stronger than those in B_{1g} geometry. The features are suppressed by applied magnetic fields, suggesting that they are indeed closely related to the gap parameter 2Δ . The temperature dependence of the peaks of the 2Δ -like features shows typical BCS-type behavior of the gap values as a function of temperature. However, the apparent values of the gap are anisotropic, and the anisotropy is more pronounced in $\text{YNi}_2\text{B}_2\text{C}$ than in $\text{LuNi}_2\text{B}_2\text{C}$. Finite Raman scattering below the gap was experimentally observed in these “conventional” superconductors. The finite scattering is intrinsic and it appears to be linear in the Raman frequency. The lack of complete suppression of the Raman response below the 2Δ peak of apparent BCS-type superconductors needs to be further addressed.

ACKNOWLEDGMENTS

We thank G. Blumberg, T. P. Devereaux, H.-L. Liu, K.-S. Park, and M. Rübhausen for help and valuable discussions. I.S.Y. and M.V.K. were partially supported under NSF Grant

No. 9705131 and through the STCS under NSF 9120000. I.S.Y. was also supported by KOSEF Grant No. 95-0702-03-01-3. S.L.C. was supported by DOE under Grant No. DEFG02-96ER45439. I.S.Y., B.K.C., and S.I.L. were sup-

ported by the Creative Research Initiative Project of the Ministry of Science and Technology, Korea. Ames Laboratory is operated by the U.S. Department of Energy by Iowa State University under Contract No. W-7405-Eng-82.

*Present address: Department of Material Science and Technology, K-JIST, 500-712, Kwangju, Korea.

- ¹C. C. Hoellwarth, P. Klavins, and R. N. Shelton, *Phys. Rev. B* **53**, 2579 (1996).
- ²L. F. Mattheiss, *Phys. Rev. B* **49**, 13 279 (1994); W. E. Pickett and D. J. Singh, *Phys. Rev. Lett.* **72**, 3702 (1994); J. I. Lee, T. S. Zhao, I. G. Kim, B. I. Min, and S. J. Youn, *Phys. Rev. B* **50**, 4030 (1994); H. Kim, C.-D. Hwang, and J. Ihm, *ibid.* **52**, 4592 (1995).
- ³L. F. Mattheiss, T. Siegrist, and R. J. Cava, *Solid State Commun.* **91**, 587 (1994).
- ⁴I. K. Yanson, V. V. Fisun, A. G. M. Jansen, P. Wyder, P. C. Canfield, B. K. Cho, C. V. Tomy, and D. McK. Paul, *Phys. Rev. Lett.* **78**, 935 (1997).
- ⁵P. C. Canfield, P.L. Gammel, and D.J. Bishop, *Phys. Today* **51** (10), 40 (1998).
- ⁶V. Metlushko *et al.*, *Phys. Rev. Lett.* **79**, 1738 (1997); V. G. Kogan, S. L. Bud'ko, P. C. Canfield, and P. Miranovic, *Phys. Rev. B* **60**, R12 577 (1999); L. Civale, A. V. Silhanek, J. R. Thompson, K. J. Song, C. V. Tomy, and D. McK. Paul, *Phys. Rev. Lett.* **83**, 3920 (1999).
- ⁷D. McK. Paul, C. V. Tomy, C. M. Aegerter, R. Cubitt, S. H. Lloyd, E. M. Forgan, S. L. Lee, and M. Yethiraj, *Phys. Rev. Lett.* **80**, 1517 (1998).
- ⁸M. R. Eskildsen, K. Harada, P.L. Gammel, A. B. Abrahamsen, N. H. Andersen, G. Ernst, A. P. Ramirez, D. J. Bishop, K. Mortensen, D. G. Naugle, K. D. D. Rathnayaka, and P. C. Canfield, *Nature (London)* **393**, 242 (1998).
- ⁹P. L. Gammel, D. J. Bishop, M. R. Eskildsen, K. Mortensen, N. H. Andersen, I. R. Fisher, K. O. Cheon, P. C. Canfield, and V. G. Kogan, *Phys. Rev. Lett.* **82**, 4082 (1999).
- ¹⁰P. Dervenagas, M. Bullock, J. Zarestky, P. Canfield, B. K. Cho, B. Harmon, A. I. Goldman, and C. Stassis, *Phys. Rev. B* **52**, R9839 (1995); H. Kawano, H. Yoshizawa, H. Takeya, and K. Kadowaki, *Phys. Rev. Lett.* **77**, 4628 (1996); C. Stassis, M. Bullock, J. Zarestky, P. Canfield, A. I. Goldman, G. Shirane, and S. M. Shapiro, *Phys. Rev. B* **55**, R8678 (1997); M. Bullock, J. Zarestky, C. Stassis, A. Goldman, P. Canfield, Z. Honda, Gen Shirane, and S. M. Shapiro, *ibid.* **57**, 7916 (1998); A. J. Arko, D. Marshall, L. W. Lombardo, A. Kapitulnik, P. Dickinson, S. Doniach, J. DiCarlo, A. G. Loeser, and C. H. Park, *Phys. Rev. Lett.* **70**, 1553 (1993).
- ¹¹G. T. Jeong, J. J. Kye, S. H. Chun, Z. G. Khim, W. C. Lee, P. C. Canfield, B. K. Cho, and D. C. Johnston, *Physica C* **253**, 48 (1995); T. Ekino, H. Fujii, M. Kosugi, Y. Zenitani, and J. Akimitsu, *Phys. Rev. B* **53**, 5640 (1996); Y. De Wilde, M. Iavarone, U. Welp, V. Metlushko, A. E. Koshelev, I. Aranson, G. W. Crabtree, and P. C. Canfield, *Phys. Rev. Lett.* **78**, 4273 (1997).
- ¹²F. Bommeli, L. Degiorgi, P. Wachter, B. K. Cho, P. C. Canfield, R. Chau, and M. B. Maple, *Phys. Rev. Lett.* **78**, 547 (1997).
- ¹³A. A. Abrikosov and V. M. Genkin, *Zh. Eksp. Teor. Fiz.* **65**, 842 (1973) [*Sov. Phys. JETP* **38**, 417 (1974)]; M. V. Klein and S. B. Dierker, *Phys. Rev. B* **29**, 4976 (1984).
- ¹⁴S. B. Dierker, M. V. Klein, G. W. Webb, and Z. Fisk, *Phys. Rev. Lett.* **50**, 853 (1983); R. Hackl, R. Kaiser, and S. Schicktzan, *J. Phys. C* **16**, 1729 (1983); R. W. Hackl, R. Kaiser, and W. Gläser, *Physica C* **162-164**, 431 (1989).
- ¹⁵R. Hackl, W. Gläser, P. Müller, D. Einzel, and K. Andres, *Phys. Rev. B* **38**, 7133 (1988); S. L. Cooper and M. V. Klein, *Comments Condens. Matter Phys.* **15**, 99 (1990); M. Krantz and M. Cardona, *J. Low Temp. Phys.* **99**, 205 (1995).
- ¹⁶M. Xu, P. C. Canfield, J. E. Ostenson, D. R. Finnemore, B. K. Cho, Z. R. Wang, and D. C. Johnston, *Physica C* **227**, 321 (1994).
- ¹⁷M. R. Eskildsen, P. L. Gammel, B. P. Barber, A. P. Ramirez, D. J. Bishop, N. H. Andersen, K. Mortensen, C. A. Bolle, C. M. Lieber, and P. C. Canfield, *Phys. Rev. Lett.* **79**, 487 (1997).
- ¹⁸V. G. Hadjiev, L. N. Bozukov, and M. G. Baychev, *Phys. Rev. B* **50**, 16 726 (1994); H.-J. Park, H.-S. Shin, H.-G. Lee, I.-S. Yang, W. C. Lee, B. K. Cho, P. C. Canfield, and D. C. Johnston, *ibid.* **53**, 2237 (1996).
- ¹⁹M. Kang, A. Bock, G. Blumberg, I.-S. Yang, and M. V. Klein (unpublished); M. Kang, Ph.D. thesis, University of Illinois, 1997.
- ²⁰M. Sera, S. Kobayash, M. Hiroi, N. Kobayashi, H. Takeya, and K. Kadowaki, *Phys. Rev. B* **54**, 3062 (1996).
- ²¹A. P. Litvinchuk, L. Börjesson, N. X. Phuc, and N. M. Hong, *Phys. Rev. B* **52**, 6208 (1995); T. Hirata and H. Takeya, *ibid.* **57**, 2671 (1998).
- ²²T. P. Devereaux and A. P. Kampf, *Int. J. Mod. Phys. B* **11**, 2093 (1997).